A physics-informed search for metric solutions to Ricci flow, their embeddings, and visualisation

Aarjav Jain, Challenger Mishra and Pietro Liò

UNIVERSITY OF CAMBRIDGE
Computer Laboratory

1 Introduction

Ricci flow is a powerful tool for geometric analysis. Intuitively, Ricci flow is a geometric flow of a metric on a smooth Riemannian manifold, which uniformizes curvature of the metric. Given a smooth Riemannian manifold $\mathcal{M}$, Ricci flow assigns a metric g to each *time* t, dictated by the Ricci tensor of the metric,

$$\partial_t g_{ab}(x,t) = -2Ric_{ab}(g(x,t)),\ where\ a,b \in \{1,2,\ldots,dim(\mathcal{M})\}. \tag{1}$$

In this work, we formulate Ricci flow on real geometries using Physics Informed Neural Networks (PINNs), where a loss function corresponding to PDE and initial condition residuals are inserted in the loss function. We focus on the real torus, and consider cigar solitonic solutions to the Ricci flow equation 1. We use PINNs to solve PDEs to embed the torus metric into R^3 to create a visualisation of the torus after Ricci Flow. Our aim is to create a framework in which to explore and visualise higher dimensional and/or complex geometries to Ricci flow problems, which do not have many analytically solved examples.

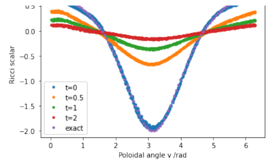

Figure 1: Ricci scalar decay with torus angle under RF

2 Experiments

In order to create a loss function, we can define a PDE residual and evaluate this for data points generated randomly on the manifold, as in Equation 2:

$$\mathcal{L}_{res}(\theta) := \frac{1}{N}\sum_{i=1}^{N} |r_\theta(t_i, x_i)|^2\,,\ with\ \ r_\theta(t,x) := \frac{\partial}{\partial t} g_\theta(t,x) + 2Ric(g_\theta(t,x)) \tag{2}$$

This can be repeated for symmetry and initial condition residual terms, and these are added to create a total loss function. A neural network minimised this function will approximate the solution to Ricci flow. Training is done using the Adam optimiser on a fully connected feed-forward network with three hidden layers of 16, 32 and 16 units, and Softplus activation. We use 1000 randomly generated training points in the metric domain.

Real Torus: The 2D square torus is parametrised by toroidal and poloidal angles, denoted by u and v respectively, with $u \in [0, 2\pi)$ and $v \in [0, 2\pi)$. Applying the torus initial conditions and the correct rotational symmetry residual terms in the loss function, the torus loss function is created and is trained. In Figures 1, we show the evolution of the scalar curvature (which is the trace of the $Ric(g)$) with the time. An MSE of the initial profile is found using the exact profile (found by differentiating the initial metric) and is $\sim 10^{-3}$ We compare the PINN generated solution with numerical simulations using a standard PDE solver in Mathematica. The computation took around 4 hours on an i5 laptop.

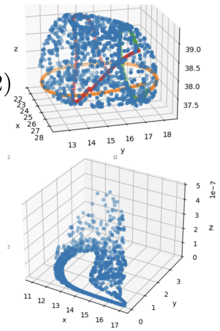

Figure 2: 3D plot of torus manifold embedded under Ricci flow. Above is initial, and below is after 2 seconds of RF

Embedding the torus: We use the metric solution for torus Ricci flow to solve Nash embedding equation to embed the torus into R^3 and plot it. The equation is:

$$g_{ij}(x) = \sum_{\alpha=1}^{n} \frac{\partial f^\alpha}{\partial x^i}\frac{\partial f^\alpha}{\partial x^j}, \alpha \in 1, 2, \ldots, n \tag{3}$$

and is solved using PINNs with an identical architecture to the torus Ricci flow. On obtaining the embeding functions, 1000 random points on the torus metric are embeded and this is plotted, shown in figure 2, We show the metric before, and after two seconds of Ricci flow. As expected, the manifold as flatter after Ricci Flow, but the expected toroidal rotational symmetry is not seen. It is found that the results depend on the magnitudes of terms in the loss function, and since the relative magnitude of terms fluctuates, an adaptive regularisation scheme can help.

Cigar soliton: A two dimensional metric with an analytic solution to the Ricci flow is the cigar soliton. It has metric $g(\mathbf{x}) = (1 + x^2 + y^2)^{-1} I_2$, with its Ricci flow solution:

$$g(t, \mathbf{x}) = (e^{4t} + x^2 + y^2)^{-1} I_2,\ where, \quad (x,y) \in R^2. \tag{4}$$

Applying the initial metric to the loss function and training, gives a PINN solution to this metric's Ricci flow, $g(t, x, y$. A plot of the $g_{11} = g_{22}$ component is shown on the top of Figure 3. The behaviour of the PINN generated solution bears close resemblance to the analytic solution, although over time, the MSE gradually grows. Minima is seen since error grows but values decrease with time.

3 Discussion

We applied a PINN technique to solve the Ricci Flow for real, 2D geometries. The solution for a torus matched well to that found by a PDE solver, and had an MSE of $\mathcal{O}(10^{-3})$ compared with the exact solution for the toroidal initial metric. The cigar soliton geometry matched the analytic solution, with an MSE of $\mathcal{O}(10^{-2})$. The learned PINN metric for torus Ricci flow was used to solve PDEs derived from the Nash–Kuiper Embedding theorem using PINNs. This allows visualisations of manifolds under Ricci Flow, showing elements of correctness.rotational symmetry was not perfectly replicated in either case, which are potentially due to compounding numerical errors during the course of Ricci flow, although the growth shows signs of stabilising. Instead of demanding rotational symmetry from the loss function, one may embed it directly with an appropriate coordinate system. This was avoided here, since choosing one can become difficult when working with larger dimensional and/or complex manifolds. Further, the magnitudes of various loss terms being important to the final embedding, an adaptive technique could be employed. The PINN approach allowed simple differentiation of the neural network solution, to find relevant quantities of Ricci tensor and curvature, as well as being beneficial in the context of Nash–Kuiper embedding. The tool we have created is completely general, and allows adaptation to the setting of real manifolds by simply changing the initial metric loss function.

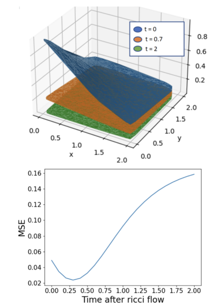

Figure 3: Cigar PINN metric and MSE plots